Chapter 5
Natural Dye-Sensitized Solar Cells: Fabrication, Characterization, and Challenges

D. Ganta, K. Combrink and R. Villanueva

Abstract Bio-inspired dye-sensitized solar cells (DSSCs) from natural plant-based dyes gained importance due to their low cost of manufacturing and environmental friendliness. Not all plants are candidates for DSCCs; they should contain certain pigments such as chlorophyll, anthocyanin, and betalains. Titanium oxide nanoparticles play an important role as electron transporter in the DSSCs. The efficiency is still low in comparison with traditional silicon-based solar cells. There are several challenges to improve the efficiency such as the photodegradation of the dye, the stability of the electrolyte over time, and adhesion of dye with titanium oxide nanoparticles. We reviewed methods for fabricating DSSCs, and the science behind the working principle. Various microscopic and spectroscopic analysis methods such as Fourier transform infrared spectroscopy and confocal microscopy were presented, for investigating optical properties, surface chemistry of the dyes, and in structural characterization of the plant cells. The photoelectrochemical properties such as conversion efficiency measure the performance of the DSSCs. They are usually in the range of 0.05–3.9% depending on the plant dye used, including plant dyes modified. A critical feature in the design of dye-sensitized solar cells is the attachment of the photosensitizing dye to the titanium oxide surface. We reviewed and summarized the design of binding elements that enhance the binding of the sensitizing dye to the titanium dioxide surface. The efficiencies of covalent linkage of the dye to the titanium surface versus non-covalent binding were discussed, including a survey of functional groups and geometries, to determine the most effective reported.

Keywords Plant dye solar cells · Titanium oxide · Nanomaterials FTIR · Photovoltaics

D. Ganta (✉) · R. Villanueva
School of Engineering, Texas A&M International University, Laredo, TX 78041, USA
e-mail: deepak.ganta@tamiu.edu

K. Combrink
Department of Biology and Chemistry, Texas A&M International University, Laredo, TX 78041, USA

H. Tyagi et al. (eds.), *Advances in Solar Energy Research*, Energy, Environment, and Sustainability, https://doi.org/10.1007/978-981-13-3302-6_5

5.1 Introduction

Energy sustainability strongly depends on utilization of renewable natural resources available such as sunlight and water, including the methods to reduce carbon dioxide emissions. Sunlight is sustainable, inexpensive, and abundant and the use of potential systems mimicking photosynthesis in the plants is underutilized. The solar energy needed to be adequately utilized to prevent pollution and global warming from other nonrenewable energy conversion methods such as coal and fossil fuels. Photovoltaic cell fabricated from silicon and thin film gained importance as first- and second-generation energy devices. The cost of manufacturing is still high and recycling the hardware after use is still a problem causing environmental pollution. There is a huge demand for organic, sustainable, and inexpensive photovoltaic devices, environmentally friendly that mimic plants in energy conversion.

In 1960s, Hishiki and others developed the DSSCs by using zinc oxide and plant dyes (Gerischer et al. 1968; Namba and Hishiki 1965). Later in 1991, Gratzel et al. developed the first DSSCs using nanocrystalline TiO_2 replacing the zinc oxide (O'Regan and Gratzel 1991). DSSCs from ruthenium were metal-based dyes and not organic; they recorded high efficiency of 11–12% (Buscaino et al. 2008; Chiba et al. 2006). They are still not environmentally friendly and not safe to handle, and platinum metal used for the cathode is also very expensive. There are three essential parts in DSSCs: cathode or counter electrode, dye, anode or working electrode, and electrolyte. Inexpensive materials such as carbon or graphite are replacing platinum. Currently, the highest efficiency reported in DSSC is 13% (Mathew et al. 2014). Initially, the majority of the dyes were chemical based, used were not green, readily available in nature or sustainable, this motivated many researchers to investigating next-generation bio-based photovoltaic devices, mimicking photosynthesis and utilizing the pigments in the dyes for DSSCs.

Plant-based DSSCs are inexpensive and nontoxic and do not cause harm to the environment in comparison with the chemical-based DSSCs. Plant dyes serve as a sensitizer, which absorbs sunlight and converts solar energy into electric energy. Several plant-based dyes were reported to be used as sensitizers in DSSCs, and the performance results were reported in Table 5.1. The maximum conversion efficiency is still lower ($\sim$3.9%) in comparison with the start-of-the-art non-plant-based or chemical-based DSSCs (13%). The ultimate goal moving forward in the natural bio-based DSSC research is to design and develop DSSCs which are stable and have high conversion efficiency comparable to the silicon-based solar cells. The pigments in the dyes such as chlorophyll, anthocyanin, and betalains are developed in the plants naturally, and it is difficult to vary the surface chemistry or be able to control it over time. Anchoring of those plant pigments to working electrode or titanium oxide film properly with strong adhesion is a significant challenge to the researchers. Researchers are now able to extract pigments of interest, modify the extraction process of the dye with solvents, be able to control the pH of the resultant dye solutions, and further be able to co-sensitize

Table 5.1 Photoelectrochemical parameters of selected natural plant dyes reported for DSSCs

Plant source	Structure	J_{sc} (mA/cm^2)	V_{oc} (V)	FF (%)	η (%)	References
Black rice	Anthocyanin	2.09	0.47	57	0.56	Noor et al. (2014)
Lawsonia inermis seed	Lawsone	2.99	0.50	70	1.47	Ananth et al. (2014)
Brown seaweed	Chlorophylls	0.8	0.36	69	0.18	Calogero et al. (2014)
Red Frangipani	Anthocyanin	0.94	0.49	65	0.30	Shanmugam et al. (2013)
Ixora sp. (Rubiaceae)	Anthocyanin	6.26	0.35	47	0.96	Kumara et al. (2013a)
Rhododendron	Anthocyanin	1.61	0.58	61	0.57	Zhou et al. (2011)
Yellow rose	Xanthophyll	0.74	0.6	57	0.26	Zhou et al. (2011)
Petunia	Chlorophyll	0.85	0.61	61	0.32	Zhou et al. (2011)
Violet	Anthocyanin	1.02	0.49	65	0.33	Zhou et al. (2011)
Rosella	Anthocyanin	1.63	0.4	57	0.37	Wongcharee et al. (2007)
Blue pea	Anthocyanin	0.37	0.37	33	0.05	Wongcharee et al. (2007)
Red Bougainvillea spectabilis	Betalain	2.29	0.28	76	0.48	Hernandez-Martinez et al. (2011)
Hibiscus rosa-sinensis	Anthocyanin	3.31	0.14	55	1.08	Yusoff et al. (2014)
Blueberry	Anthocyanin	4.1	0.3	55	0.69	Teoli et al. (2016)
Tangerine peel	Flavone	0.74	0.59	63	0.28	Zhou et al. (2011)
Fructus lycii	Carotene	0.53	0.68	46	0.17	Zhou et al. (2011)
Mangosteen pericarp	∝-Mangostin/ β-mangostin	2.55	0.62	58	0.92	Zhou et al. (2011)
Wild Sicilian prickly pear	Etalain	8.20	0.38	38	1.19	Calogero et al. (2010)
Nephelium lappaceum (F: Sapindaceae)	Anthocyanin	3.88	0.41	35	0.56	Kumara et al. (2013b)
Mulberry fruit	Anthocyanin	1.89	0.56	49	0.55	Chang and Lo (2010)
Ivy gourd fruits	β-carotene	0.24	0.64	49	0.08	Wongcharee et al. (2007)
Codiaeum variegatum	Anthocyanin	4.03	0.44	55	1.08	Yusoff et al. (2014)
Ipomoea	Chlorophyll	0.91	0.54	56	0.28	Chang et al. (2010)
Rhoeo spathacea	Chlorophyll, carotenoids	10.9	0.5	27	1.49	Lai et al. (2008)
Red cabbage	Anthocyanin	2.25	0.62	70	0.97	Chien and Hsu (2014)

(continued)

Table 5.1 (continued)

Plant source	Structure	J_{sc} (mA/cm^2)	V_{oc} (V)	FF (%)	η (%)	References
Pandan leaves	Chlorophyll	1.91	0.48	56	0.51	Noor et al. (2014)
Spinach	Modified chlorophyll/ neoxanthin	11.8	0.55	60	3.9	Wang et al. (2006)
Aloe vera	Anthocyanin	0.11	0.67	50	0.38	Ganta et al. (2017)
Cladode of cactus	Chlorophyll	0.24	0.64	48	0.74	Ganta et al. (2017)

the TiO_2 film, all of which lead to an improvement in the performance of the natural plant-based DSSCs (Hug et al. 2014; Kumara et al. 2017).

A critical feature in the design of dye-sensitized solar cells is the attachment of the photosensitizing dye to the titanium oxide surface. The effort was devoted to exploring the structural features needed for efficient dye-sensitized solar cells (Hagfeldt et al. 2010). Despite the vast variety of structures for the donor–π-bridge–acceptor motifs of organic dye-sensitized molecules, there are a small set of acceptor groups used in the dyes. The acceptor portion of the dye serves several critical functions. The first is to participate in the transfer of electrons in the donor–acceptor motif to facilitate the rapid charge transfer of the hole to the redox mediator and the second is to bind to the titanium oxide layer to facilitate the transfer of charge into the titanium oxide conduction band. The binding of the dye to the titanium layer should be strong and should favor the formation of a tightly packed monolayer that is devoid of aggregates. The most common acceptor functional group is a carboxylic acid which has several common binding modes (Hagfeldt et al. 2010). The binding mode of the carboxylic acid was determined by analysis of the carbonyl (C=O) stretch frequency as well as the O–C–O asymmetric stretch of the carboxylic acid (Hagfeldt et al. 2010).

In this chapter, we discuss and review methods reported to develop natural plant-based DSSCs and the challenges in the surface adhesion chemistry. In Sect. 5.2, we discuss the structure and operation of the DSSCs and the science behind it followed by Sect. 5.3 where we will discuss the methods used in the fabrication of DSSCs. In Sect. 5.4, we review the challenges in the adhesion of plant dye in the DSSCs, comparing covalent versus intermolecular bonding in the dyes, and a discussion on the solvent systems which will aid the adsorption of the dye onto TiO_2. In Sect. 5.5, we will discuss various analytical methods used for characterization of the plant dye, including characterization of its interaction with titanium oxide; followed by methods and results on testing the performance of the DSSCs in Sect. 5.6. In Sects. 5.7 and 5.8, we conclude with a summary or discussion on the future direction and perspectives.

5.2 Structure and Operating Principle of DSSCs

There are four main components in TiO_2-based natural plant dye solar cells: (1) conducting oxide (CO) glass slide coated with monocrystalline titanium oxide film (working electrode or anode), (2) counter electrode or cathode (carbon or platinum coated conductive glass), (3) plant dye, and (4) electrolyte. In this section, we will discuss the science involved in them to operate as a simple DSSCs. The nanoscale TiO_2 nanopowder in the form of a film coated on the conducting glass slide and the glass slide is immersed in the plant dye solution for the proper amount of time to dye the TiO_2 film properly. Here, the electrolyte which contains (I_3^-/I^-) acts as a redox mediator in the entire operation of the DSSCs. The plant dyes should have the required chemical bonds to anchor such as carboxyl group to attach onto the TiO_2 film. Figure 5.1 shows the schematic diagram of the components in DSSCs.

The entire operation involves transport of electrons generated by absorption of photons from sunlight through the photoexcitation of the plant dye. Plant dye absorbs photons from sunlight; electrons are generated from the photoexcitation of the plant dye. Electrons were further energized enough to move from highest energy occupied molecular orbital (HOMO) to lowest energy occupied molecular orbital (LUMO). The difference between HOMO and LUMO has a more significant

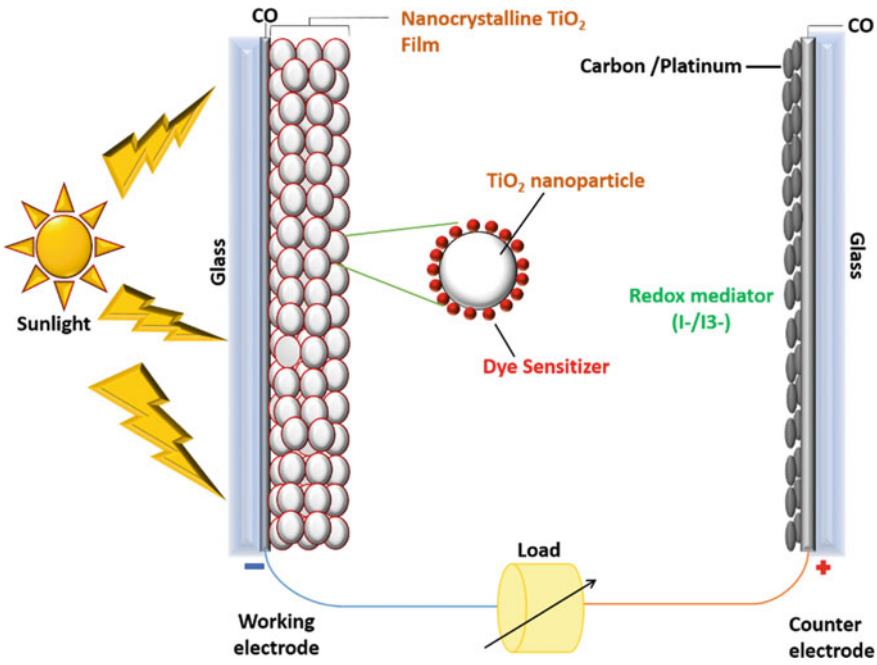

Fig. 5.1 Schematic of the structure of the DSSCs

influence on the absorption properties, including the range of the absorption of the plant dye. Electrons then jump or transport to the conduction band (CB) of TiO_2 and are further transported further via TiO_2 nanoparticles mesh through an external load to reach the cathode, thereby completing the electrical circuit, leading to the conversion of energy from sunlight to electric energy.

It is crucial that the LUMO energy level of the dye be higher than the energy of the (CB) of TiO_2 and the HOMO should also be lower than the redox potential of the electrolyte used. It is also crucial to have a uniform and crack-free TiO_2 coating on the surface of a conductive glass slide. The final step in the operation of DSSCs is the dye regeneration as the result of oxidation of the dye; electrolyte plays a vital role in supplying the required electrons from the I^- ions. Figure 5.2 shows a simplified schematic illustrating the operation principle of DSSCs.

There are also challenges involved in the undesirable recombination processes involving electrons generated and oxidized dye within the dye, trying to hinder the electron transport but that process is not kinetically favorable to dominate the regular electron transport (Ning et al. 2010; Preat et al. 2010; Meng et al. 2008; Maurya et al. 2016; Maiaugree et al. 2015). The efficiency of the DSSC is strongly dependent on the electron transport kinetics happening at the interfaces across of the main components of the DSSCs. Conversion efficiency is highly dependent on the anchoring groups, electrolyte, cathode material, and anode material. Band structure (especially bandgap between HOMO and LUMO) also plays a vital role in the absorption of the sunlight. LUMO energy level of the dye not being higher than

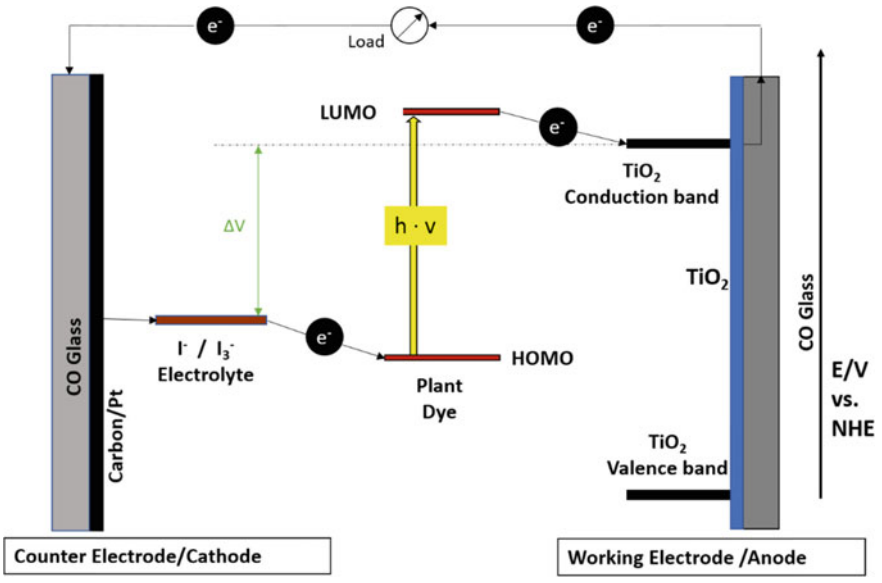

Fig. 5.2 Schematic of the operation of the DSSCs, describing the energy levels and electron transfer from the anode to cathode across various interfaces such as dye–TiO_2 and electrolyte–dye

the energy of the conduction band (CB) reduces the overall conversion efficiency. In summary, the electron generation, electron transport, and dye regeneration are three crucial steps in the operation of the DSSCs.

5.3 Methods of Fabrication of DSSCs

In this section, we would discuss the selection of the plant dye, fabrication methods reported in the assembly of the DSSCs, with an example on how we assembled the DSSC with the cladode (*nopal*) of the prickly pear cactus (*optunia ficus–indica*) plant dye.

5.3.1 Selection and Preparation of the Natural Dye Sensitizers

Natural plant-based dyes are inexpensive, nontoxic, environmentally friendly, and readily available. The dyes are usually extracted through a cost-effective and straightforward process mostly from the flowers and leaves of the plants. The color of the dye depends on the pigments present in the dye such as chlorophyll, anthocyanin, and betalains. The plant dyes should have absorption in the visible or near-infrared region in order to be suitable for energy conversion.

Figure 5.3 shows a simple design of the dye which acts as a photosensitizer. A π bridge connects the donor and acceptor part of dye and has donor and acceptor

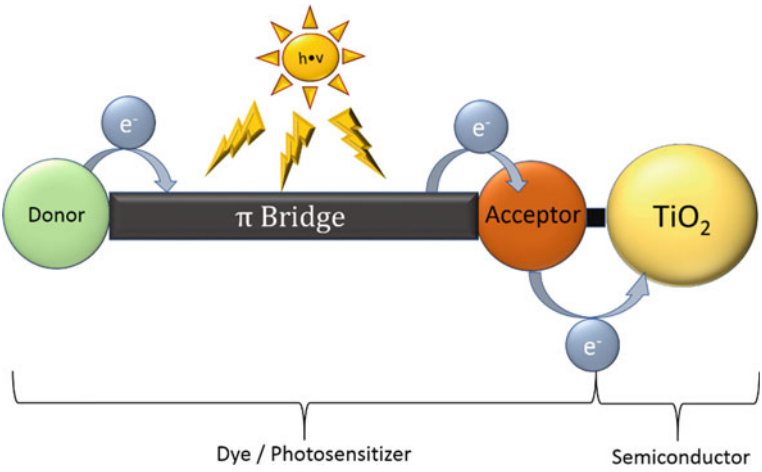

Fig. 5.3 Simple design (donor–π–acceptor) structure of the dye

part for electrons. The functional groups present in the dye which anchor to the TiO_2 are present on the acceptor part of the dye. The chemical adsorption or adhesion of the natural dyes on the surface of the TiO_2 film occurs due to the presence of the anchoring functional groups present in the dye such as hydroxyl (–OH) groups, esters, and carbonyl (C=O) groups (Meng et al. 2008; Maurya et al. 2016; Maiaugree et al. 2015). For example, in the case of anthocyanin molecule, it binds with TiO_2 via carbonyl and hydroxyl groups; these anchors transfer the electrons from the photo-excited dye to TiO_2 film.

There are several methods reported where dyes are either modified, mixed to form a cocktail or used in the side-by-side configuration, including several factors which must be taken into account such as pH of the plant dye extract solution (Hug et al. 2014; Kumara et al. 2017; Teoli et al. 2016). Figure 5.4 shows a simple schematic of the chemical structure of the selective dyes most commonly used in DSSC fabrication, anthocyanin, β-mangostin, and chlorophyll a. Instability of the plant-based dye under exposure to sunlight is a significant concern. Two steps were considered, including solar cell assembly under an inert atmosphere and protection from sunlight, and still, they do not last more than a year (Hug et al. 2014; Calogero et al. 2012). One of the quick solutions for the problem would be to find ways to add new dye or exchange it with similar or another dye without disturbing the adhesion of the dye to TiO_2. Another approach would be to find ways to modify the surface chemistry of the dye to prevent photodecay while the efficiency is varied over time. In nature, plant and other biological species can regrow the pigments internally as they get damaged, and the damaged ones get replaced, without any external support.

The inexpensive and straightforward plant dye extraction procedures for cladodes of prickly pear cactus are discussed. First, the cladodes are cleaned and rinsed with water. Next, small pieces of them were blended in a blender until we were able to obtain a liquid natural plant dye solution. The plant dye is diluted with ethanol to give a final ratio of ethanol to dye of 1:1. The plant dye solutions were further filtered to remove any solid residue present in the solution. The dye can decay over time under exposure to sunlight. In the next step, care was taken to cover the dye with aluminum foil and stored in the refrigerator to prevent any contamination or photodecay. We have attempted to image the cells in the plant dye using confocal microscopy, upon excitation with a light source of 500–560 nm, as illustrated in Fig. 5.5. The information on the cells structural integrity can be beneficial in the design of DSCCs, thereby improving their efficiency. The dye is clear and ready for use, as illustrated in Fig. 5.6. The plant dyes are usually used within 48 h. Still, systematic study needed to be conducted to investigate how chemical bonds change with time under exposure to the sunlight over a period of few hours or months to estimate the lifetime of the cell.

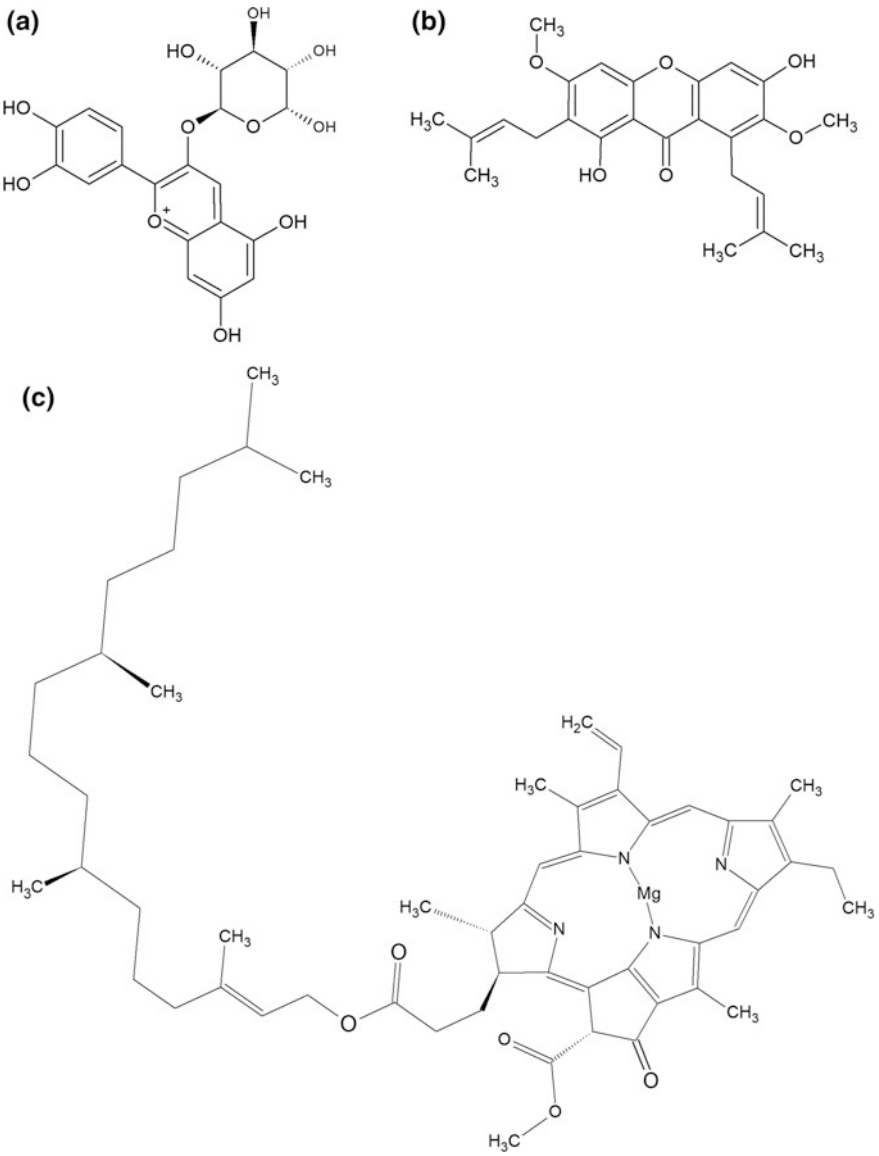

Fig. 5.4 Chemical structure of the most commonly used dye classes: **a** cyanin (an anthocyanin), **b** β-mangostin, **c** chlorophyll a

5.3.2 Working Electrode and Fabrication Method

TiO_2 is the choice of semiconductor material used for photoelectrode in the DSSCs. It is nontoxic, inexpensive, and can be handled safely. The nanopowder of TiO_2 is

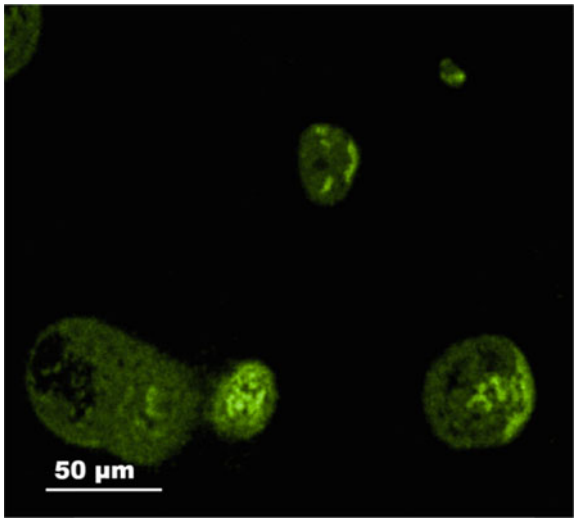

Fig. 5.5 Confocal microscopy image of the cells present in a plant dye (cladode) used for DSSCs

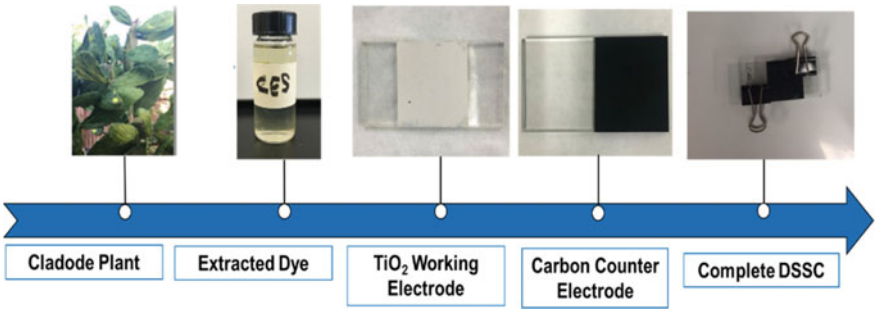

Fig. 5.6 Steps in the fabrication of DSSCs from the extraction of cladode, to the complete assembly of the solar cell

used to increase the surface area for natural dye absorption. The LUMO of many dyes is compatible with TiO_2. TiO_2 is also available in a crystalline form to increase the surface area. Usually, X-ray diffraction methods are used to test the crystallinity (anatase) for the in-house prepared nanopowder. Other conditions which are met by TiO_2 include having high carrier mobility to be able to collect the photoelectrons efficiently. Other materials such as zinc oxide, stannic oxide, and magnesium oxide are used for the working electrode fabrication (Fukai et al. 2007; Sakai et al. 2013; Kumara et al. 2004).

For the fabrication of the working electrode, transparent CO glass was chosen with right resistance; in our case, we have chosen fluorine-doped tin oxide (FTO) glass with a sheet resistance of 14 Ω/sq obtained commercially. FTO glass is cleaned to ensure no impurities or contaminants on the surface using acetone and ethanol in an ultrasonic bath and preheated to test for cracking. Next, a thin film of TiO_2 was deposited from nanopowder paste using a combination of blade and tape casting to ensure proper height and uniformity, followed by annealing at a high temperature of around 390 °C. It is essential to ensure that there is no aggregation in the TiO_2 particles. The coating should be uniform without any cracks and nicely spread over the conductive side of the FTO glass slide, and the nonconductive side left for the electrical contact.

The titanium oxide-coated FTO glass is then immersed in the plant dye, inside a petri dish and left undisturbed for ~24 h and the petri dish is covered to prevent any photodecay of the dye. The immersion time of the natural dye plays a vital role in the performance of the DSSCs, and we should ensure the titanium oxide film is dyed correctly by observing the color change on the surface by simple inspection.

5.3.3 Preparation of Counter Electrode

The requirements for a counter electrode or cathode include being a good conductor, electron donor to the oxidized electrolyte reducing it with low overvoltage, low resistance to charge transport, entire surface should be able to respond to charge transport, and highly stable under the influence of light over time (Kumara et al. 2017). In summary, the triiodide is formed from the plant dye reduced at the cathode.

The materials used for the counter electrode are platinum and carbon. Although platinum is a better material as a counter electrode for reduction reaction and most commonly used for electrochemistry experiments, carbon or graphite coating is inexpensive, readily available in many forms and easy to handle. The conductive glass slide is coated with the material of choice, in our case we used carbon or graphite, and FTO glass slides cleaned in an ultrasonic bath with acetone and ethanol for 10 min.

The conductive glass is simply burned with an electric lighter to form a nice and uniform coating of carbon black on the surface. The carbon coating should be stable and adhered correctly to the glass slide and not washed out in the presence of an electrolyte. Another method is to either deposit carbon soot or paint the conductive glass with colloidal graphite (Ghann et al. 2017). The platinum electrode is prepared by the sputtering method, where a thin film of platinum is deposited on the surface of the conductive glass slide, and the thickness of the film can be controlled (Hug et al. 2014; Kumara et al. 2017; Maiaugree et al. 2015).

5.3.4 Electrolyte Preparation and Assembly of DSSCs

The primary function of the electrolyte is the redox reaction, where the electron is transferred from the electrolyte to the oxidized dye, to complete the dye regeneration process. There are three type of electrolytes usually used for DSSCs, liquid, solid, and quasi-solid and should have properties such as (1) nontoxic and noncorrosive, (2) high ionic/electrical conductivity, (3) does not photodegrade, (4) good contact with both monocrystalline TiO_2 on one side and counter electrode on the other side, and (5) does not react with either dye or electrodes and lead to unwanted byproducts from the chemical reaction. The most widely used electrolyte is iodide–triiodide (I^-/I_3^-). The lack of stability and the need to refill the electrolyte in the DSSCs over time is still a significant issue in the development of DSSCs.

We prepared the electrolyte solution from 0.5 M potassium iodide, 0.5 M iodine, water, and ethylene glycol. Both counter and working electrodes are brought closer and held together with clips with a tiny gap in between for the electrolyte solution. Finally, using a pipette or a dropper electrolyte, drops are injected into the tiny gap between the electrodes. Proper care must be taken to ensure the electrolyte gently seeps inside the cell upon injection into the small space between the electrodes, filling it entirely with the capillary action. Visual inspection must be done to ensure there is either no carbon black washout or titanium oxide nanoparticles removed and dissolved in the electrolyte. Figure 5.6 shows the simple illustration of the steps involved in the DSSCs fabrication. The main steps in the development of DSSCs, as shown in the figure, include extraction of the dye, titanium oxide working electrode fabrication, carbon counter electrode fabrication, and assembly of working and counter electrode together sandwiched with electrolyte in between them.

5.4 Dye Adsorption on Titanium Oxide and Challenges

5.4.1 Covalent Versus Intermolecular Bonding Dyes

Catechols are the most common anchoring group found in natural product-derived sensitizing dyes. The anchoring group can mimic mussel adhesion proteins that can bind strongly to a variety of surfaces including wet surfaces (Sidharam et al. 2014). Electron-withdrawing groups added to the catechol can be used to tune the bond strength. However, this approach has not been widely used in dye solar cells (Sidharam et al. 2014). Four binding modes are possible including several hydrogen bonding arrangements, chelative, and binuclear dentate binding (Fig. 5.7) (Sidharam et al. 2014).

For synthetic dyes, the most common acceptor–anchoring functional groups are the carboxylic acid and the cyanoacrylate groups (Hagfeldt et al. 2010). In examples where a direct comparison can be made, the cyanoacrylate anchor gave slightly

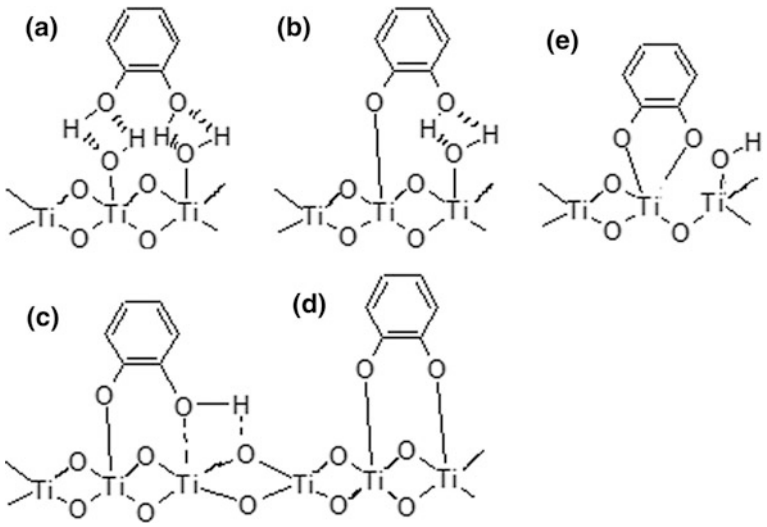

Fig. 5.7 Binding modes for catechols (Sidharam et al. 2014). **a** Hydrogen bonding, **b** monodentate w/bridging hydrogen bonding, **c** binuclear bidentate, **d** chelative bridging, **e** bidentate chelating

better solar cell efficiency than the carboxylic acid (Prauzner-Bechcicki et al. 2016a). Dyes with acids are typically soaked with the titanium dioxide layer in a polar aprotic solvent such as THF or CH_3CN (Sidharam et al. 2014). This procedure often gives initial weak hydrogen bonding interaction with the titanium dioxide surface (Sidharam et al. 2014). Heating after adsorption can improve the stability of the binding due to the formation of bidentate adsorption (Fig. 5.8) (Sidharam et al. 2014). As was observed in the catechol dyes, the electron-withdrawing nitrile is likely contributing stronger binding due to increased acidity of the acrylic acid in this system. Carboxylic acids have several documented binding modes (Hagfeldt et al. 2010; Sidharam et al. 2014; Murakoshi et al. 1995). The binding mode achieved is dependent on the conditions used for the adsorption process (Sidharam et al. 2014). A hydrogen bonding arrangement is often first formed between the carboxylic acid and the titanium dioxide surface that can be further strengthened by heating the adsorbed acid to form an ester-like bond to the TiO_2 surface (Sidharam et al. 2014). In an example with a porphyrin dye using scanning probe microscopy, the orientation of the dye changes from a flat orientation to an edge orientation on heating (Prauzner-Bechcicki et al. 2016a).

It cannot be assumed that the polar acceptor groups are the only functional groups interacting with the titanium dioxide surface. Pretreating the titanium nanoparticles with nitric acid has been reported to reduce the time required for adsorption when compared to conventional soaking methods (Kim et al. 2013). Although the dye adsorption process was faster, the stability over time was similar (Kim et al. 2013). Several papers explore adding a second or third acceptor–anchoring system, and in some cases, the multi-anchored systems do show

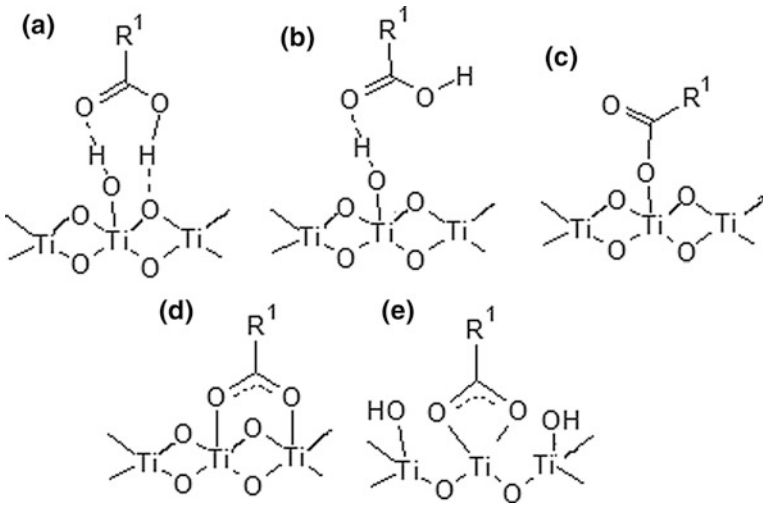

Fig. 5.8 Binding modes of carboxylate groups to metal oxides (Sidharam et al. 2014). **a** Hydrogen bonding to the bridging oxygen, **b** hydrogen bonding to the carbonyl oxygen, **c** monodentate methyl ester, **d** bidentate bridging, **e** bidentate chelating

enhanced efficiency when compared to the single-anchor systems (Lee et al. 2016; Song et al. 2018). In other systems, there is no trend toward multi-anchor systems being superior (Chen and Lin 2017). Aggregation of the dye can limit the efficiency of the binding, and some compounds showed improved binding due to the addition of branched or aliphatic chains to limit aggregation (Song et al. 2018). The study also explored the aqueous stability of nine representative dyes. The nine compounds represented only the carboxylic acid and cyanoacrylate acceptor–anchoring groups. In this study, the superior binding compound in the aqueous solution used a carboxylic acid anchor, but the authors noted that the lipophilicity of the compounds due to added alkyl side chains away from the carboxylic acid anchor played a role in the added stability due to reduced aggregation (Song et al. 2018).

Since nonaqueous electrolyte solutions are commonly used, poor stability in aqueous solution may not necessarily be a fatal flaw for a dye-sensitized molecule. A study looking at multi-anchoring sensitizers indicated that di- and tri-anchored dyes had better long-term stability (Lee et al. 2016). In this study, the electrolyte solution was a nonaqueous ionic liquid with lithium iodide–iodine system and an acetonitrile/valeronitrile as a solvent (Lee et al. 2016). The triple-anchored dye was reported to be stable to desorption in concentrated aqueous KOH solution which the authors speculated would result in an improved lifetime of the cell (Lee et al. 2016). The acceptor–anchoring group in this study was the cyanoacrylate, and the authors showed with IR data that the cyano group did not contribute to the binding of the dye to the titanium dioxide layer (Lee et al. 2016). A study looking at several porphyrin derivatives by scanning probe microscopy found that the binding mode varied from the edge on to a flat-lying geometry depending on how the dye is

attached to the titanium dioxide layer (Prauzner-Bechcicki et al. 2016a). This study demonstrates that the conditions and solvent used to adsorb the dye to the titanium dioxide substrate are critical for determining the binding mode, efficiency, and possibly the longevity of the cell (Prauzner-Bechcicki et al. 2016a).

Dye adsorption conditions vary from several hours at room temperature (Hagfeldt et al. 2010) to elevated temperatures for one to several hours at temperatures ranging from 50 to 80 °C (Prauzner-Bechcicki et al. 2016a). Dye aggregation can also be addressed by using coadsorbents such as chenodeoxycholic acid (cheno) and deoxycholic acid usually directly in the dye solution during the adsorption process (Sidharam et al. 2014). The coadsorbant in cases where aggregation is not a problem can limit the amount of dye loading which may reduce the efficiency of the system (Sidharam et al. 2014).

Some effort has been devoted to finding additional acceptor groups that have a high affinity for the titanium dioxide layer. Most of the functional group acceptor studies used a porphyrin motif for the dye (Higashino et al. 2017; Tomohiro et al. 2015, 2017). Non-covalent titanium-binding acceptors such as tropolone, 8-hydroxyquinoline, hydroxamic acid, pyridine, and phosphinic acid anchoring groups have been reported (Higashino et al. 2017; Tomohiro et al. 2015, 2017; He et al. 2012; Ismael et al. 2012; Kakiage et al. 2015; Mai et al. 2015).

Infrared (IR) spectroscopy is the primary tool for determining the binding mode for acceptor groups. For the tropolone derivative, the binding mode is reported as bidentate as evidenced by broadening of the OH and C=O stretches in the IR spectra of the unbound and bound forms of the acceptor indicating a symmetrical bidentate binding mode (Tomohiro et al. 2015). A similar observation is reported for the hydroxamic acids with the hydroxy IR peak disappearing and the C=O peak shifting to low wavenumbers indicating the formation of a bidentate keto form of the hydroxamic acid (Tomohiro et al. 2017). Both papers also report that the compounds are very strongly bound to silica gel which eliminates silica gel chromatography as a method for purification. Three pyridine acceptors were evaluated and had several possible binding modes (Mai et al. 2015). The unsubstituted 4-pyridyl derivative can directly interact with the metal in a Lewis acid–base interaction or through a hydrogen bonding interaction with the oxide metal surface and the Lewis basic pyridine nitrogen. Both binding modes are monodentate (Mai et al. 2015). A second 2-pyridone (2-hydroxypyridine) motif takes advantage of pyridones ability to form a bidentate ligand based on the pyridine nitrogen and the pyridone oxygen acting as a Lewis base that can interact with the titanium metal surface (Mai et al. 2015). The third pyridine derivative is a 2-carboxypyridine that acts as carboxylic acid and does not appear to involve the pyridine nitrogen in the binding mode resulting in the normal carboxylic acid binding with no evidence for ester formation with the titanium oxide surface (Mai et al. 2015). A pyridine ring is more electron deficient than a benzene ring resulting in a strong binding interaction with good long-term stability (Mai et al. 2015). A phosphinic acid anchoring group has also been described as a new anchoring group (Ismael et al. 2012). The phosphinic acid group was a tight binder to the titanium dioxide which translated to better long-term stability. The authors noted some aggregation issues that were

improved with coadsorption with cheno with a slight enhancement in efficiency despite lower sensitizer binding.

A slightly different approach has been reported with a silyl anchor that forms a covalent bond to the titanium surface (Higashino et al. 2017; Kakiage et al. 2015). The propargyl silyl group gave the fastest surface coverage while the aryl silyl groups required (Ghann et al. 2017) hours to reach constant surface coverage. The conditions used to attach the silane to the surface were critical as well as the ethanol solution gave poor results while a mixture of toluene/acetonitrile (9/1) gave the best results (Higashino et al. 2017). A comparison of a carboxylic acid derivative versus the silyl adsorped anchor showed impressive retention of the dye in aqueous solution with the silyl groups remaining after 7 h in an aqueous solution (Higashino et al. 2017). The second series of silyl anchored dyes were reported using a diphenylamine and indazole donor-based dyes (Kakiage et al. 2015). Both silyl compounds showed similar improvements in dye adsorption when compared to their carboxylic acid and cyanoacrylate analogs (Higashino et al. 2017; Kakiage et al. 2015).

All of the anchoring group explorations did not significantly improve the efficiency of the devices. The tighter binding compounds, as well as the covalently linked compounds, appear to improve the stability of the devices significantly. A robust screening method to determine the strength of binding to a titanium dioxide substrate could allow more rapid screening of additional functional groups that could be used as anchoring groups. Titanium dioxide affinity columns have been reported to be useful for enriching samples with phosphorylated proteins (Engholm-Keller and Larsen 2011). Although commercial titanium dioxide chromatography columns do not exist, a thin layer system should provide a quick screening method to explore additional anchoring groups and different solvent systems that could be used to improve dye binding. New anchoring groups have focused on known metal binding groups such as hydroxamic acids, 8-hydroxyquinolines, 2-hydroxypyridines, phosphinic acids, and tropolones. Acid isosteres such as sulfonamides, sulphonic acids, acyl sulfonamides, tetrazoles, or covalent linkers such as a phosphoramidite have not been explored. These groups could be screened for titanium dioxide binding efficiency quickly, and the strongest binders could be incorporated into current or new dyes. A similar approach was used to measure the protein binding for drug candidates (Cheng et al. 2004). This method uses an HPLC column with human albumin-bound as the stationary to estimate the binding of compounds based on the retention time of the compounds on this chromatography column and compounds with known binding values and retention times (Cheng et al. 2004).

Dyes for solar cells are typically dissolved in water, or a polar organic solvent such as chloroform, ethanol, acetonitrile, dimethyl sulfoxide (DMSO), dimethylformamide (DMF), or supercritical carbon dioxide and titanium dioxide coated plates are dipped or soaked in these solutions for various amounts of time depending on the dye used. The solvent used, time, and method of soaking vary and

are critical for the effective formation of the dye titanium dioxide interface (Song et al. 2018; Rajab 2016; Tedla and Tai 2018; Tian et al. 2008). Since most dyes rely on hydrogen bonding or dipole interactions with the titanium dioxide layer for adsorption, solvents that do not compete with the dye for titanium dioxide binding would be expected to have the most extended cell life. Water is a poor solvent choice for the electrolyte solution because desorption of the dye commonly observed with carboxylic acid acceptors (Tian et al. 2008). Several researchers report that polar aprotic solvents give better adsorption than polar protic solvents like methanol or ethanol (Sidharam et al. 2014; Tian et al. 2008; Ali Shah et al. 2017). For this reason, the electrolyte solution is often different from the solution used to adsorb the dye to the titanium dioxide surface. Polar aprotic solvents such as chloroform, acetonitrile, or a higher boiling valeronitrile were often used alone, or in combination with polyethylene glycol (PEG), ion liquids (1,2-dimethyl-3-propylimidazolium iodide or 1-butyl-3-methylimidizoliumbromide), or 4-tert-butylpyridine for the electrolyte solution in dye-sensitized solar cells (Prauzner-Bechcicki et al. 2016a; Higashino et al. 2017; Nurrisma et al. 2017).

5.4.2 Solvent Systems for Dye Absorption

The solvent choice and time for the adsorption process influence the amount of dye adsorbed, the type of bonding achieved, and the stability of the deposited monolayer obtained (Sidharam et al. 2014; Rajab 2016; Tedla and Tai 2018; Tian et al. 2008; Prauzner-Bechcicki et al. 2016b). Since the key binding modes of acceptors rely on hydrogen bonding or dipole–dipole interactions, solvents that can also bind to the titanium dioxide layer using these binding modes will decrease the binding efficiency of the dye for the titanium dioxide layer, thus reducing efficiency and durability of the system. A solvent is also necessary to allow the electrolyte to interact with the plant dye in the recycle process. The electrolyte solvent must solvate the electrolyte system as well as maintain the dye monolayer on the titanium surface. Modest improvements in the efficiency of DSSCs have been made, but less effort has been devoted to DSSCs long-term stability. Recent reports of stronger titanium dioxide binding acceptor groups as well as new covalent dye TiO_2 anchors indicate that progress is being made to improve the long-term stability of these new solar cells.

5.5 Analysis Methods

In this section, we would provide a brief overview of the commonly used methods to test the natural plant dye and the TiO_2 film.

5.5.1 Characterization of the Dye

It is important to test the dye for its optical properties and chemical structure, if it is suitable for the fabrication of the DSSCs and the two methods used for that purpose are optical absorption and Fourier transform infrared spectroscopy (FTIR). If the solution is dilute which is the case for dye solution, absorbance is then described by the Beer–Lambert Law:

$$A = \varepsilon(\lambda)CL \tag{5.1}$$

where L is the path length in cm, A is the absorbance, C is the molar concentration of the material absorbing (dye in our case) in M, and $\varepsilon(\lambda)$ is the extinction coefficient or molar absorptivity in cm^{-1} M^{-1}, strongly dependent on the wavelength of the light or laser used.

Figure 5.9 illustrates the UV–Vis absorption spectra obtained in the wavelength range of 500–800 nm for the dye ethanol extracts of cladode. A stronger absorption peak at 662 nm was observed for the cladode extract, confirming the presence of chlorophyll. Similarly, for aloe vera dye extract, an absorption peak was observed at 524 nm, a signature showing the presence of anthocyanins. Normally, strong absorption peaks were seen near-visible and near-infrared region for plant dyes used in the DSSCs.

While absorption spectra verify the presence of the right pigments present in the dye, we need to verify the presence of the chemical bonds or anchors needed for adhesion onto the TiO_2 film, and for that purpose, FTIR spectroscopy technique is used. The fundamental principle behind FTIR is that several wavelengths or frequencies of infrared light are incident or exposed on the sample; some of the light is absorbed by the sample, and rest is transmitted and molecular fingerprint of the

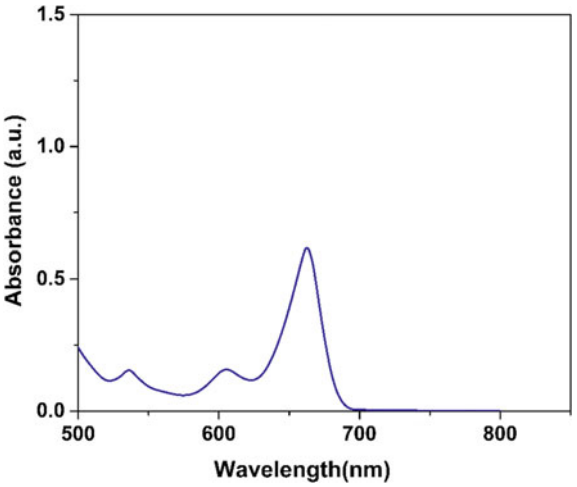

Fig. 5.9 Absorption spectra in the UV–Vis region of the natural plant dye and ethanol extracts of cladode of prickly pear

sample for various chemicals from the signal data. The raw data is proceeded further using Fourier transform algorithm to get the FTIR spectra (wavenumber vs. intensity). Absorption means there is a match between the frequency of incident light and vibrational frequency of the molecule. The spectra are then compared with the existing library from the software for various chemical bonds to find a match and identify the chemical bonds present on the surface. Thus details on the surface chemistry can be obtained.

FTIR spectra were obtained for both the aloe vera and cladode plant dye extracts in the range of 2800–3500 cm^{-1}, showing the presence of hydroxyl functional group (3300 cm^{-1}). Carbonyl groups and ester functional groups (1050 cm^{-1}) and other functional groups are also shown, but these are most important for serving as anchors for adhesion onto the TiO_2 film. There is variation in the peak intensities for both dyes that differ at different frequencies as both of them have different chemical structures associated with the presence of different plant pigments. FTIR results also support the absorption spectroscopy results, which verifies the presence of anthocyanin and chlorophyll pigment molecules. Figure 5.10 shows the illustration of the FTIR spectra for the cladode dye.

5.5.2 *Characterization of the Titanium Oxide and Dye*

It is essential to perform structural analysis of the TiO_2 nanopowder in order to be suitable for working electrode fabrication. A simple scanning electron microscopy (SEM) images can show if there is aggregation in the titanium oxide nanopowder, but they do not provide high-resolution imaging information with atomic resolution, and the defects in the crystalline planes and the interfaces cannot be obtained. The crystallinity of the TiO_2 nanopowder could be verified from the X-ray powder

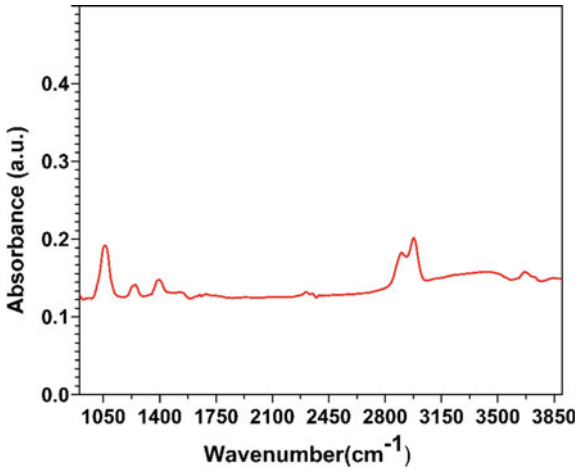

Fig. 5.10 FTIR of the dye ethanol extracts of the cladode of prickly pear (Ganta et al. 2017)

diffraction method. The size of the nanoparticles of TiO_2 can be obtained from high-resolution transmission electron microscopy (HR-TEM) method, including the in situ information on crystallography with the selected area electron diffraction (SAED) method. Majority of the TEMs can obtain SAED patterns or diffraction rings with the inbuilt feature. SAED technique can obtain information on the defects in the crystalline planes and the grain boundaries.

There is a need to study the interaction with the dye, as the dye molecules decorate the TiO_2 nanoparticles. The HR-TEM images reported showed the interaction between the pomegranate dye and TiO_2 nanoparticles, including the information on their lattice planes, d-spacing, and the interaction between the TiO_2 nanoparticles and the dye, which could be the result of hydroxyl-containing dye being deprotonated or transfer of proton (Ghann et al. 2017).

5.6 Performance of the DSSCs

The DSSCs are illuminated under standard AM 1.5 standard sunlight; it depended on the beam characteristics and intensity was measured from the irradiance measurements, using a simple irradiance meter. Current density versus voltage (*J-V*) curve is obtained upon illumination of the DSSC sample from a sun simulator using a potentiostat. Five main parameters govern the performance of DSSCs and described in detail:

(1) Short-circuit current density (J_{sc}): It is the photocurrent incident on the sample per unit area in mA/cm^2. The values are obtained from a *J-V* curve as shown in Fig. 5.11 for the cladode-based DSSC. The strength of current density is dependent on the strong interaction between the sunlight, dye and TiO_2, and the absorption coefficient of the dye. Higher current densities usually lead to higher

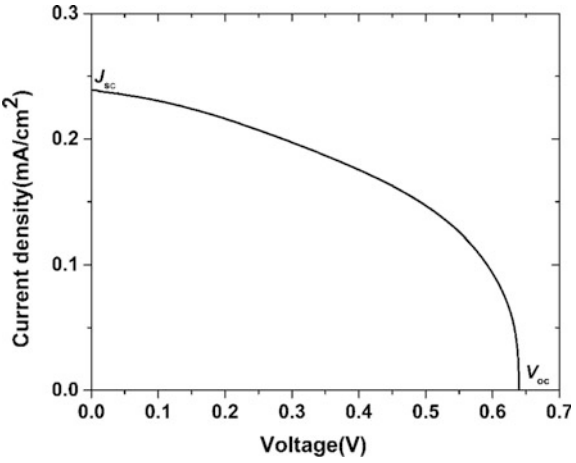

Fig. 5.11 The *J-V* curve for the cladode DSSC, measured under the illumination from the sun simulator, indicating open-circuit voltage (V_{oc}) and short-circuit current density (J_{sc}) along the *y*- and *x*-axes, respectively (Ganta et al. 2017)

light-to-energy conversion efficiency. In the case of natural plant-based DSSCs, the J values do vary with time as the plant dye losses its stability or they photodecay over time, and several groups are investigating on finding a solution for the problem.

(2) Open-circuit voltage (V_{oc}): The open-circuit voltage values can be obtained in the J-V curve when the solar cell is illuminated when the circuit is open. A rough estimate of the voltages can be obtained by simply measuring the solar cell in sunlight with a multimeter and under darkness it should not give any voltage values. It can also be obtained from the following expression given by (Kumara et al. 2017).

$$V_{oc} = \frac{E_{cb}}{e} + \frac{K_b T}{e} \ln\left(\frac{n}{N_{cb}}\right) - \frac{E_{redox}}{e} \tag{5.2}$$

where K_b is the Boltzmann constant, T is the absolute temperature, e is the charge, n is the number of electrons in the conduction band, E_{cb} is the energy of the conduction band, E_{redox} is the redox potential, and N_{cb} is the density of the states in the conduction band.

(3) Fill factor (FF): Fill factor is defined as the ratio of the maximum power ($J_{max} \cdot V_{max}$) and the product of open-circuit voltage and current density. The values are obtained from the J-V curve and is given by,

$$FF = \frac{V_{max} \cdot J_{max}}{J_{sc} \cdot V_{oc}} \tag{5.3}$$

The maximum value of the FF is unity, and the unsuccessful fabrication of the DSSCs can lead to a reduced value.

(4) Photovoltaic energy conversion efficiency (n): This is an important parameter to test for the successful fabrication of the DSSCs, verifying if the dye was suitable for DSSCs. The first step would be to test the solar cell in darkness, showing no energy conversion efficiency; the solar cell was illuminated with sunlight from sun simulator and the parameters in the J-V curve and F; we can calculate the energy conversion efficiency. The expression for efficiency is given by,

$$n = \frac{J_{sc} \cdot V_{oc} \cdot FF}{I_{inc}} \tag{5.4}$$

where I_{inc} is the incident light intensity or irradiance usually measured from the incident light source, usually it is measured to be either 100 mW/cm^2 or intensity can be reduced to 100 W/m^2 with appropriate optics. The beam from a sun simulator usually diverges and it is recommended to perform the measurement with a circular beam and by placing the DSSCs closer to the sun simulator.

The photoelectrochemical parameters of the selected dye DSSCs are listed in Table 5.1. The efficiencies are usually in the range of 0.05–3.9% based on the plant dye and modified plant dyes used for fabrication of DSSCs. It also includes our reported experimental data. Strong adhesion of dye molecules on TiO_2, uniform coating of the TiO_2 film, plays a vital role in the efficiency of the DSSCs.

(5) Incident photon-to-current conversion efficiency (IPCE): It is also referred to as external quantum efficiency and the measurement checks on how efficient the conversion of photons to electrons occurs at various wavelengths. It also gave information on the stability of the solar cell over time. The monochromator is used to select a specific wavelength from the monochromatic sunlight source before being incident on the DSSC. The standard expression for it is given by,

$$\mathrm{IPCE}(\%) = \frac{1240 \cdot J_{\mathrm{sc}}}{I_{\mathrm{inc}} \cdot \lambda} \tag{5.5}$$

where λ is the wavelength of the monochromatic light incident on the DSSCs.

5.7 Perspective and Challenges

In future, three significant issues lower efficiency, the stability of the plant dye over time, and an electrolyte which needs to be refilled over time needed to be addressed for the DSSCs to be commercialized. Research is needed on ways to modify the plant dyes chemical structure or functionalize them in order to prevent the photodecay from UV rays; experimentally, we can filter out the UV rays, but in reality, natural sunlight does have UV rays, and it is impossible to avoid them. Another option would be to discover new plant dyes extracted from various parts of the plant not reported to be used for DSSCs, but that option is challenging given the amount of literature reported on the usage of almost all of the plant dyes readily available. A cocktail of dyes, a combination of the dye in the side-by-side configuration without mixing them and also the addition of graphene to the dye, did not provide a boost in the conversion efficiency (Ganta et al. 2017; San Esteban and Enriquez 2013; Chang et al. 2013).

Another major issue is the lack of the choice of electrolytes used for the DSSCs assembly. Research is needed on the discovery of novel electrolytes which are compatible with both the plant dye and TiO_2 film in the charge transport without comprising on the efficiency. The electrolytes should not be volatile under the exposure to the sun or decay with time. Temperature changes also affect their electrolyte stability as they expand due to stress causing leakage from the DSSCs. Integration of electrolyte inside the DSSCs is another major issue with limited spacing between the cathode and anode to accommodate the electrolyte and the difficulty in covering the entire area between them for better interaction.

Finally, the low efficiency of the DSSCs is a significant concern in comparison with silicon and metal-based DSSCs. Proper selection of materials for dyes, electrolyte, cathode, and anode, including the discovery of new materials for that purpose, was required in future to improve the energy conversion efficiency. Materials such as graphene provided a boost in efficiency when used as an additive, but still, the materials research needs additional work. The interaction between the materials is also essential to study the energy transport kinetics. Designing a heterojunction DSSCs of various materials might be able to provide a boost in the efficiency by taking advantage of different materials, controlling the optical properties such as absorption and further be able to engineer the energy levels and the bandgaps, and minimizing the recombination reactions.

5.8 Conclusions

In summary, the methods and results presented in this chapter on DSSCs were reported using natural plant-based dyes as sensitizers. The dyes were extracted from parts of the plant and carefully analyzed both microscopy and spectroscopy methods as discussed in Sect. 5.4. Detailed discussion on the surface chemistry of the plant dye upon interaction with the TiO_2 film is also presented, including discussion on the various anchoring groups involved in the process. It was studied that adhesion promoters or anchoring groups played an important role in solar energy conversion, by helping in adsorption of the dye onto TiO_2 film, leading to improved light-to-energy conversion. In Sect. 5.6, the photoelectrochemical performance of the DSSCs is determined by the conversion efficiency and are in the range of 0.05–3.9% depending on the plant dye used and design of the solar cell.

The lower cost and environmental friendliness make DSSCs strong candidates for green energy, and they respond to very low-intensity sunlight and not dependent on the intensity of the sunlight or the angle of the incidence. In future, with improvements in the efficiency and stability over time, DSSCs can be integrated into the wearable devices especially in textiles and also occupy very low area making them suitable to be used on building for light-to-energy conversion, especially in big cities where space is major concern.

Acknowledgements The TAMIU faculty startup funds and U.S. National Science Foundation (Award number: 17268800) supported this work. We would also like to thank Luis Carrasco and Carlos Guzman for assisting in electrode fabrication and the selection of materials.

References

Ali Shah Z, Zaib KMK, Qureshi M (2017) Dye sensitized solar cells based on different solvents: comparative study, 07

Ananth S, Vivek P, Arumanayagam T, Murugakoothan P (2014) Natural dye extract of lawsonia inermis seed as photo sensitizer for titanium dioxide based dye sensitized solar cells. Spectrochim Acta Part A Mol Biomol Spectrosc 128:420–426

Buscaino R, Baiocchi C, Barolo C, Medana C, Grätzel M, Nazeeruddin MK, Viscardi G (2008) A mass spectrometric analysis of sensitizer solution used for dye-sensitized solar cell. Inorg Chim Acta 361(3):798–805

Calogero G, Di Marco G, Cazzanti S, Caramori S, Argazzi R, Di Carlo A, Bignozzi CA (2010) Efficient dye-sensitized solar cells using red turnip and purple wild sicilian prickly pear fruits. Int J Mol Sci 11(1):254

Calogero G, Yum J-H, Sinopoli A, Di Marco G, Grätzel M, Nazeeruddin MK (2012) Anthocyanins and betalains as light-harvesting pigments for dye-sensitized solar cells. Sol Energ 86(5):1563–1575

Calogero G, Citro I, Di Marco G, Armeli Minicante S, Morabito M, Genovese G (2014) Brown seaweed pigment as a dye source for photoelectrochemical solar cells. Spectrochim Acta Part A Mol Biomol Spectrosc 117:702–706

Chang H, Lo Y-J (2010) Pomegranate leaves and mulberry fruit as natural sensitizers for dye-sensitized solar cells. Sol Energ 84(10):1833–1837

Chang H, Wu HM, Chen TL, Huang KD, Jwo CS, Lo YJ (2010) Dye-sensitized solar cell using natural dyes extracted from spinach and ipomoea. J Alloy Compd 495(2):606–610

Chang H, Kao M-J, Chen C-H, Chen C-H, Cho K-C, Lai X-R (2013) Characterization of natural dye extracted from wormwood and purple cabbage for dye-sensitized solar cells. Int J Photoenerg 2013:1–8

Chen Y-C, Lin JT (2017) Multi-anchored sensitizers for dye-sensitized solar cells. Sustain Energ Fuels 1(5):969–985

Cheng Y, Ho E, Subramanyam B, Tseng J-L (2004) Measurements of drug–protein binding by using immobilized human serum albumin liquid chromatography–mass spectrometry. J Chromatogr B 809(1):67–73

Chiba Y, Islam A, Watanabe Y, Komiya R, Koide N, Han L (2006) Dye-sensitized solar cells with conversion efficiency of 11.1%. Jpn J Appl Phys 45(7L):L638

Chien C-Y, Hsu B-D (2014) Performance enhancement of dye-sensitized solar cells based on anthocyanin by carbohydrates. Sol Energ 108:403–411

Engholm-Keller K, Larsen MR (2011) Titanium dioxide as chemo-affinity chromatographic sorbent of biomolecular compounds—applications in acidic modification-specific proteomics. J Proteomics 75(2):317–328

Fukai Y, Kondo Y, Mori S, Suzuki E (2007) Highly efficient dye-sensitized SnO_2 solar cells having sufficient electron diffusion length. Electrochem Commun 9(7):1439–1443

Ganta D, Jara J, Villanueva R (2017) Dye-sensitized solar cells using aloe vera and cladode of cactus extracts as natural sensitizers. Chem Phys Lett 679:97–101

Gerischer H, Michel-Beyerle ME, Rebentrost F, Tributsch H (1968) Sensitization of charge injection into semiconductors with large band gap. Electrochim Acta 13(6):1509–1515

Ghann W, Kang H, Sheikh T, Yadav S, Chavez-Gil T, Nesbitt F, Uddin J (2017) Fabrication, optimization and characterization of natural dye sensitized solar cell. Sci Rep-Uk 7:41470

Hagfeldt A, Boschloo G, Sun L, Kloo L, Pettersson H (2010) Dye-sensitized solar cells. Chem Rev 110(11):6595–6663

He H, Gurung A, Si L (2012) 8-Hydroxylquinoline as a strong alternative anchoring group for porphyrin-sensitized solar cells. Chem Commun 48(47):5910–5912

Hernandez-Martinez AR, Estevez M, Vargas S, Quintanilla F, Rodriguez R (2011) New dye-sensitized solar cells obtained from extracted bracts of Bougainvillea Glabra and Spectabilis Betalain pigments by different purification processes. Int J Mol Sci 12(9):5565

Higashino T, Nimura S, Sugiura K, Kurumisawa Y, Tsuji Y, Imahori H (2017) Photovoltaic properties and long-term durability of porphyrin-sensitized solar cells with silicon-based anchoring groups. ACS Omega 2(10):6958–6967

Hug H, Bader M, Mair P, Glatzel T (2014) Biophotovoltaics: natural pigments in dye-sensitized solar cells. Appl Energ 115:216–225

Ismael L-D, Mingkui W, Robin H-B, Mine I, Victoria M-D, Nazeeruddin MK, Tomás T, Michael G (2012) Molecular engineering of zinc phthalocyanines with phosphinic acid anchoring groups. Angewandte Chemie Int Ed 51(8):1895–1898

Kakiage K, Aoyama Y, Yano T, Oya K, Fujisawa J-I, Hanaya M (2015) Highly-efficient dye-sensitized solar cells with collaborative sensitization by silyl-anchor and carboxy-anchor dyes. Chem Commun 51(88):15894–15897

Kim B, Park SW, Kim J-Y, Yoo K, Lee JA, Lee M-W, Lee D-K, Kim JY, Kim B, Kim H, Han S, Son HJ, Ko MJ (2013) Rapid dye adsorption via surface modification of TiO_2 photoanodes for dye-sensitized solar cells. ACS Appl Mater Interfaces 5(11):5201–5207

Kumara GRA, Okuya M, Murakami K, Kaneko S, Jayaweera VV, Tennakone K (2004) Dye-sensitized solid-state solar cells made from magnesiumoxide-coated nanocrystalline titanium dioxide films: enhancement of the efficiency. J Photochem Photobiol, A 164(1):183–185

Kumara NTRN, Ekanayake P, Lim A, Liew LYC, Iskandar M, Ming LC, Senadeera GKR (2013a) Layered co-sensitization for enhancement of conversion efficiency of natural dye sensitized solar cells. J Alloy Compd 581:186–191

Kumara NTRN, Ekanayake P, Lim A, Iskandar M, Ming LC (2013b) Study of the enhancement of cell performance of dye sensitized solar cells sensitized with Nephelium lappaceum (F: Sapindaceae). J Sol Energ Eng 135(3):031014

Kumara NTRN, Lim A, Lim CM, Petra MI, Ekanayake P (2017) Recent progress and utilization of natural pigments in dye sensitized solar cells: a review. Renew Sustain Energ Rev 78:301–317

Lai WH, Su YH, Teoh LG, Hon MH (2008) Commercial and natural dyes as photosensitizers for a water-based dye-sensitized solar cell loaded with gold nanoparticles. J Photochem Photobiol A 195(2):307–313

Lee YH, Yun HJ, Choi SK, Yang YS, Park T, Ahn K-S, Suresh T, Kim JH (2016) Triphenylamine-based tri-anchoring organic dye with enhanced electron lifetime and long-term stability for dye sensitized solar cells. Synth Met 217:248–255

Mai C-L, Moehl T, Hsieh C-H, Décoppet J-D, Zakeeruddin SM, Grätzel M, Yeh C-Y (2015) Porphyrin sensitizers bearing a pyridine-type anchoring group for dye-sensitized solar cells. ACS Appl Mater Interfaces 7(27):14975–14982

Maiaugree W, Lowpa S, Towannang M, Rutphonsan P, Tangtrakarn A, Pimanpang S, Maiaugree P, Ratchapolthavisin N, Sang-Aroon W, Jarernboon W (2015) A dye sensitized solar cell using natural counter electrode and natural dye derived from mangosteen peel waste. Sci Rep-Uk 5:15230

Mathew S, Yella A, Gao P, Humphry-Baker R, Curchod BFE, Ashari-Astani N, Tavernelli I, Rothlisberger U, Nazeeruddin MK, Grätzel M (2014) Dye-sensitized solar cells with 13% efficiency achieved through the molecular engineering of porphyrin sensitizers. Nat Chem 6:242

Maurya IC, Srivastava P, Bahadur L (2016) Dye-sensitized solar cell using extract from petals of male flowers Luffa cylindrica L. as a natural sensitizer. Opt Mater 52:150–156

Meng S, Ren J, Kaxiras E (2008) Natural dyes adsorbed on TiO_2 nanowire for photovoltaic applications: enhanced light absorption and ultrafast electron injection. Nano Lett 8(10):3266–3272

Murakoshi K, Kano G, Wada Y, Yanagida S, Miyazaki H, Matsumoto M, Murasawa S (1995) Importance of binding states between photosensitizing molecules and the TiO_2 surface for efficiency in a dye-sensitized solar cell. J Electroanal Chem 396(1):27–34

Namba S, Hishiki Y (1965) Color sensitization of zinc oxide with cyanine dyes1. J Phys Chem 69 (3):774–779

Ning Z, Fu Y, Tian H (2010) Improvement of dye-sensitized solar cells: what we know and what we need to know. Energ Environ Sci 3(9):1170–1181

Noor MM, Buraidah MH, Careem MA, Majid SR, Arof AK (2014) An optimized poly(vinylidene fluoride-hexafluoropropylene)–NaI gel polymer electrolyte and its application in natural dye sensitized solar cells. Electrochim Acta 121:159–167

Nurrisma P, Silviyanti SNA, Gatut Y (2017) Endarko, effect of mixing dyes and solvent in electrolyte toward characterization of dye sensitized solar cell using natural dyes as the sensitizer. IOP Conf Ser Mater Sci Eng 214(1):012022

O'Regan B, Gratzel M (1991) A low-cost, high-efficiency solar cell based on dye-sensitized colloidal TiO_2 films. Nature 353(6346):737–740

Prauzner-Bechcicki JS, Zajac L, Olszowski P, Jöhr R, Hinaut A, Glatzel T, Such B, Meyer E, Szymonski M (2016a) Scanning probe microscopy studies on the adsorption of selected molecular dyes on titania. Beilstein J Nanotechnol [Online] 7:1642–1653

Prauzner-Bechcicki JS, Zajac L, Olszowski P, Jöhr R, Hinaut A, Glatzel T, Such B, Meyer E, Szymonski M (2016b) Scanning probe microscopy studies on the adsorption of selected molecular dyes on titania. Beilstein J Nanotechnol 7:1642–1653

Preat J, Jacquemin D, Perpete EA (2010) Towards new efficient dye-sensitised solar cells. Energ Environ Sci 3(7):891–904

Rajab FM (2016) Effect of solvent, dye-loading time, and dye choice on the performance of dye-sensitized solar cells. J Nanomater 2016:8

Sakai N, Miyasaka T, Murakami TN (2013) Efficiency enhancement of ZnO-based dye-sensitized solar cells by low-temperature $TiCl_4$ treatment and dye optimization. J Phys Chem C 117 (21):10949–10956

San Esteban ACM, Enriquez EP (2013) Graphene–anthocyanin mixture as photosensitizer for dye-sensitized solar cell. Sol Energ 98:392–399

Shanmugam V, Manoharan S, Anandan S, Murugan R (2013) Performance of dye-sensitized solar cells fabricated with extracts from fruits of ivy gourd and flowers of red frangipani as sensitizers. Spectrochim Acta Part A Mol Biomol Spectrosc 104:35–40

Sidharam PP, Luc S, Marcelis TM, Han Z (2014) Covalent surface modification of oxide surfaces. Angewandte Chemie Int Ed 53(25):6322–6356

Song H, Liu Q, Xie Y (2018) Porphyrin-sensitized solar cells: systematic molecular optimization, coadsorption and cosensitization. Chem Commun 54(15):1811–1824

Tedla A, Tai Y (2018) Influence of binary solvent system on the stability and efficiency of liquid dye sensitized solar cells, 358

Teoli F, Lucioli S, Nota P, Frattarelli A, Matteocci F, Carlo AD, Caboni E, Forni C (2016) Role of pH and pigment concentration for natural dye-sensitized solar cells treated with anthocyanin extracts of common fruits. J Photochem Photobiol A 316:24–30

Tian H, Yang X, Chen R, Zhang R, Hagfeldt A, Sun L (2008) Effect of different dye baths and dye-structures on the performance of dye-sensitized solar cells based on triphenylamine dyes. J Phys Chem C 112(29):11023–11033

Tomohiro H, Yamato F, Kenichi S, Yukihiro T, Seigo I, Hiroshi I (2015) Tropolone as a high-performance robust anchoring group for dye-sensitized solar cells. Angew Chem Int Ed 54(31):9052–9056

Tomohiro H, Yuma K, Ning C, Yamato F, Yukihiro T, Shimpei N, Packwood DM, Jaehong P, Hiroshi I (2017) A hydroxamic acid anchoring group for durable dye-sensitized solar cells incorporating a cobalt redox shuttle. ChemSusChem 10(17):3347–3351

Wang X-F, Matsuda A, Koyama Y, Nagae H, Sasaki S-I, Tamiaki H, Wada Y (2006) Effects of plant carotenoid spacers on the performance of a dye-sensitized solar cell using a chlorophyll derivative: enhancement of photocurrent determined by one electron-oxidation potential of each carotenoid. Chem Phys Lett 423(4):470–475

Wongcharee K, Meeyoo V, Chavadej S (2007) Dye-sensitized solar cell using natural dyes extracted from rosella and blue pea flowers. Sol Energy Mater Sol Cells 91(7):566–571

Yusoff A, Kumara NTRN, Lim A, Ekanayake P, Tennakoon KU (2014) Impacts of temperature on the stability of tropical plant pigments as sensitizers for dye sensitized solar cells. J Biophys 2014:8

Zhou H, Wu L, Gao Y, Ma T (2011) Dye-sensitized solar cells using 20 natural dyes as sensitizers. J Photochem Photobiol A 219(2):188–194